Cyclic compression increases F508 Del CFTR expression in ciliated human airway epithelium

Nadzeya Marozkina,[1] Jürgen Bosch,[1] Calvin Cotton,[1] Laura Smith,[1] James Seckler,[1]
Khalequz Zaman,[1] Shagufta Rehman,[2] Ammasi Periasamy,[2] Herbert Gaston,[3] Ghaith Altawallbeh,[1]
Michael Davis,[7] David R. Jones,[4] Robert Schilz,[6] Scott H. Randell,[5] and Benjamin Gaston[1,8]

[1]Pediatric Pulmonology Division, Department of Pediatrics, Case Western Reserve University School of Medicine, Cleveland, Ohio; [2]W. M. Keck Center for Cellular Imaging, Department of Biology, University of Virginia, Charlottesville, Virginia; [3]Lake Effect Pharma, LLC, Gates Mills, Ohio; [4]Thoracic Surgery Service, Memorial Sloan Kettering Cancer Center, New York, New York; [5]Department of Cell Biology and Physiology, University of North Carolina, Chapel Hill, North Carolina; [6]Pulmonology and Critical Care Medicine University Hospitals, Cleveland, Ohio; [7]Department of Pediatrics, Division of Pulmonary Medicine, Children's Hospital of Richmond at Virginia Commonwealth University, Richmond, Virginia; and [8]Pediatric Pulmonology Division, Rainbow Babies and Children's Hospital, Cleveland, Ohio

Marozkina N, Bosch J, Cotton C, Smith L, Seckler J, Zaman K, Rehman S, Periasamy A, Gaston H, Altawallbeh G, Davis M, Jones DR, Schilz R, Randell SH, Gaston B. Cyclic compression increases F508 Del CFTR expression in ciliated human airway epithelium. *Am J Physiol Lung Cell Mol Physiol* 317: L247–L258, 2019. First published May 22, 2019; doi:10.1152/ajplung.00020.2019.— The mechanisms by which transepithelial pressure changes observed during exercise and airway clearance can benefit lung health are challenging to study. Here, we have studied 117 mature, fully ciliated airway epithelial cell filters grown at air-liquid interface grown from 10 cystic fibrosis (CF) and 19 control subjects. These were exposed to cyclic increases in apical air pressure of 15 cmH$_2$O for varying times. We measured the effect on proteins relevant to lung health, with a focus on the CF transmembrane regulator (CFTR). Immunoflourescence and immunoblot data were concordant in demonstrating that air pressure increased F508Del CFTR expression and maturation. This effect was in part dependent on the presence of cilia, on Ca^{2+} influx, and on formation of nitrogen oxides. These data provide a mechanosensory mechanism by which changes in luminal air pressure, like those observed during exercise and airway clearance, can affect epithelial protein expression and benefit patients with diseases of the airways.

airway cilia; airway clearance; airway pressure; cystic fibrosis; *S*-nitrosocysteine

INTRODUCTION

Airway epithelial cilia clear secretions and inhaled particles from the lungs (7, 47). Additionally, airway cilia have sensory functions, as do cilia in the kidney, ear, and elsewhere (13, 14, 30, 36, 39, 54). Specifically, they sense chemical stimuli (such as bitter taste agonists) (30, 36) and mechanical stimuli (such as air movement) (6, 60). Exercise and a variety of airway clearance procedures increase air pressure gradients across the ciliated airway epithelial surface (27, 48, 62). Clinically, meth-

ods that change transepithelial pressure may benefit certain patients with airways diseases, such as asthma and cystic fibrosis (CF) (4, 45). In asthma, increased airway pressure may dilate airways because of the intrinsic mechanical properties of airway smooth muscle (35). In CF and other lung diseases, ATP release associated with ciliary motion may benefit patients by augmenting airway hydration through purinergic receptors (8). However, these potential mechanisms underlying the benefits of airflow and pressure are challenging to study in detail. This is, in part, because each pseudostratified epithelial culture takes 5–6 wk per experiment to grow and because standardized and commercial systems are not yet available for air pressure and flow experiments in vitro. Here, we have studied the effect of changes in air pressure to signal changes in airway epithelial protein expression, signaling mediated, in part, by nitrogen oxides.

Whereas inducible nitric oxide synthase (iNOS) is expressed constitutively in the normal human airway epithelium (3, 34), high levels of expression are not observed for any NOS isoform in CF airway epithelial cells (33). Low-level expression of endothelial NOS (eNOS) has been reported in ciliated cell basal bodies (64, 67), and a functional role for airway eNOS is suggested by the fact that eNOS$^{-/-}$ mice have greater airway methacholine responsiveness following antigen sensitization than do inducible (iNOS)$^{-/-}$ or neuronal (nNOS)$^{-/-}$ mice (11). Of note, eNOS is activated by calcium flux that leads to calmodulin binding (25). Calcium flux through the transient receptor potential vanilloid 4 (TRPV4) channel is established to occur during airway epithelial ciliary motion (1, 39). Therefore, we hypothesized that mechanical stimulation of airway cilia could activate ciliated cell eNOS by increasing apical calcium flux.

Activation of eNOS can signal bioactivities by producing nitric oxide (NO) or *S*-nitrosothiols; alternatively, it can form inert end products such as nitrate (5, 23, 25, 40, 41, 58). The distribution and bioactivities of these chemical NOS products are regulated by colocalized proteins (5, 23, 41, 58). *S*-nitrosothiols can have a number of beneficial airway effects (2, 10, 22, 23, 26, 28, 29, 37, 40, 42, 61, 65, 66). These include airway

smooth muscle relaxation and increased cilia beat frequency. S-nitrosoglutathione (GSNO) and other S-nitrosothiols also increase expression (28, 29, 42, 65) and function (10) of the CFTR protein. However, the absence of iNOS (33), as well as impaired eNOS activity, in the CF airway appears to result in impaired GSNO production (26). Indeed, these low levels suggest that inhibiting GSNO catabolism may be futile as a therapy. We hypothesized that airway ciliary mechanotransduction could increase nitrogen oxide production and, in turn, CFTR expression.

MATERIALS AND METHODS

Reagents

All reagents were purchased from Sigma Aldrich (St. Louis, MO) unless otherwise noted.

Cell Cultures

Primary human airway pseudostratified epithelial cell cultures were grown at air-liquid interface (ALI) from bronchial (lung transplant or lobectomy) or nasal epithelial cells obtained from patients homozygous for F508Del CFTR or without CF [wild type (WT)] as previously described (9, 18, 42). Primary cells purchased from Charles River (company near our institution in Cleveland) from donors at the University of North Carolina (UNC) were also grown at ALI with minor modifications (19). These cultures were derived from subjects at UNC under the UNC Institutional Review Board (see below). These cells are annotated as in Table 1 (ALI 1–9). Additionally, CF bronchial epithelial cells (CFBE41o⁻), F508del or WT-transfected, were a gift from Dr. Eric Sorcher and grown as previously described (42, 66).

Ex Vivo Human Airway Epithelial Preparations

Tumor-free human bronchi obtained at operative lobectomy (24) were transported in lactated Ringer's solution on wet ice. A subepithelial blister was raised with sterile saline, dissected sharply (see Fig. 1A), plated on human fibronectin cellware culture slides (BD Biosciences), and incubated at least 72 h (21% oxygen-5% CO_2, 37°C) in UNC medium (18) with daily medium changes before permeabilization, staining, and imaging.

Cyclic Compressive Stress Procedures

In situ cyclic compressive stress (CCS) for microscopy is described in the immunofluorescence section. For the remainder of the studies, the ciliated, lumenal side of primary human airway pseudostratified epithelial cells in six-well transwell plates was ventilated through a sealed manifold (Fig. 1C) using a humidified rodent ventilator circuit (New England Medical Instruments, Medway, MA) at pressures 20/5 cm water and a frequency of 14 breaths per minute (in a 37°C, 21% oxygen-5% CO_2). The pressures represent "middle range" transepithelial (mucosal-to-submucosal) pressure gradient of 15 cm water (27, 48, 62); not as high as with dramatic transluminal pressures observed in asthma, but above pressures predicted during quiet breathing. Control cells in the same incubator were not attached to the ventilator. In the initial biochemical experiments, CCS was delivered similarly but as described by Button and coworkers (9). In selected experiments, CCS was also performed after a 2-h preincubation with the TRPV4 inhibitor HC067047 (500 nM) or the NOS inhibitor nitro-L-arginine methyl ester (10 mM L-NAME; Cayman Chemical, Ann Arbor, MI).

Immunofluorescence

Primary human airway pseudostratified epithelial cells and ex vivo human airway epithelia were fixed in 4% paraformaldehyde for 20 min, permeabalized in 0.05% Triton X-100 for 5 min, rinsed in phosphate buffered saline (PBS) three times (5 min), incubated overnight with primary antibodies, rinsed again in PBS three times (5 min), incubated 30 min with secondary antibodies, and then mounted with mount media and visualized by confocal microscopy (customized Zeiss equipment) (42, 53). The primary antibodies were mouse anti-eNOS mAB (BD Transduction Laboratories; 1:200 dilution), rabbit anti-eNOS pAB (Cell Signaling; 1:200 dilution), and mouse anti-Dynein MAB (Thermo Scientific; 1:200). DAPI was from ThermoScientific. The isotype controls were Purified Rabbit IgG Isotype Standard (no. 550875; BD Biosciences) and Purified Mouse IgG1 κ Isotype Control (no. 557273; BD Biosciences). The secondary antibodies were Alexa Fluor 488 chicken anti-mouse (Invitrogen; 1:500 dilution) and Alexa Fluor 568 goat anti-rabbit (Invitrogen; 1:250 dilution). In separate experiments at UNC, an Olympus FV10000 confocal microscope was used to image eNOS (Ab PA3031A; ThermoFisher; 1:200) in whole mount cells using donkey anti-rabbit AlexaFluor 488 (1:1,000) secondary (Ab 715-545-151; Jackson ImmunoResearch). Normal rabbit IgG was used as a control (5 μg/ml; Ab 550875; BD Biosciences). Cells were also stained with phalloidin for filamentous actin (Phalloidin Alexa 647; Invitrogen; 1:50) as well as for cilia (rat anti-tubulin MAB1864; 3 μg/ml; Millipore) (donkey anti-rat; Ab 712-295-153; Jackson ImmunoResearch; 1:1,000). DNA was imaged with Hoescht 33342 (0.01 mg/ml; H1399; Invitrogen).

Imagestream

Psuedostratified WT and F508/F508 ALI cultures grown at 30°C for 72 h or at 37°C and treated with CCS as above for 0, 0.5, 2, or 3 h. Cells were removed from filters with Accutase and calcium/magnesium-free PBS (1 mM EDTA) treatment for 10 min at 37°C. Released cells were then fixed in 4% paraformaldehyde in PBS (final concentration) in solution for 15 min at 4°C using mild agitation on an Eppendorf rotator. The paraformaldehyde-treated cells were incubated with primary and secondary antibodies as follows: CFTR (RB7865; 1:5,000; Ref. 67); eNOS (BD Transduction Laboratories; 1:500); AF488 anti-rabbit (Molecular Probes; 1:15,000) AF546 anti-mouse (Molecular Probes; 1:15,000); and DRAQ5 (Cell Signaling; 1:10,000). Only cells treated with anti-eNOS were permeabilized with 0.2% Triton X-100 for 15 min (room temperature). After incubation with the secondary antibodies, cells were visualized on ImageStream X Mark II (lasers set to the following powers: 488 nm = 50 mW, 658 nm = 60 mW, and 768 nm = 3.5 mW). Compensation matrices were collected for DRAQ5 and unstained cells to account for their autofluorescence and applied throughout the analysis. About 50% of the cells were in focus based on gradient root mean square analysis of the bright-field for further evaluation. The focused cells were then separated by aspect ratio and area observed in the DRAQ5 channel, allowing the identification of single versus multiple cells based on

Table 1. *Sources and cystic fibrosis genotypes and growth for the human pseudostratified bronchial epithelial cell cultures grown at air-fluid interface*

Annotation	Genotype/No.	Source
ALI 1	F508/F508-1	Charles River
ALI 2	F508/F508-2	UNC
ALI 3	F508/F508-3	Charles River
ALI 4	WT-1	Charles River
ALI 5	WT-2	UNC
ALI 6	WT-3	CWRU
ALI 7	WT-4-6	UVA
ALI 8	F508/F508-4	CWRU
ALI 9	WT-7	CWRU

ALI, air-liquid interface; WT, wild type; UNC, University of North Carolina, Chapel Hill; CWRU, Case Western Reserve University; UVA, University of Virginia.
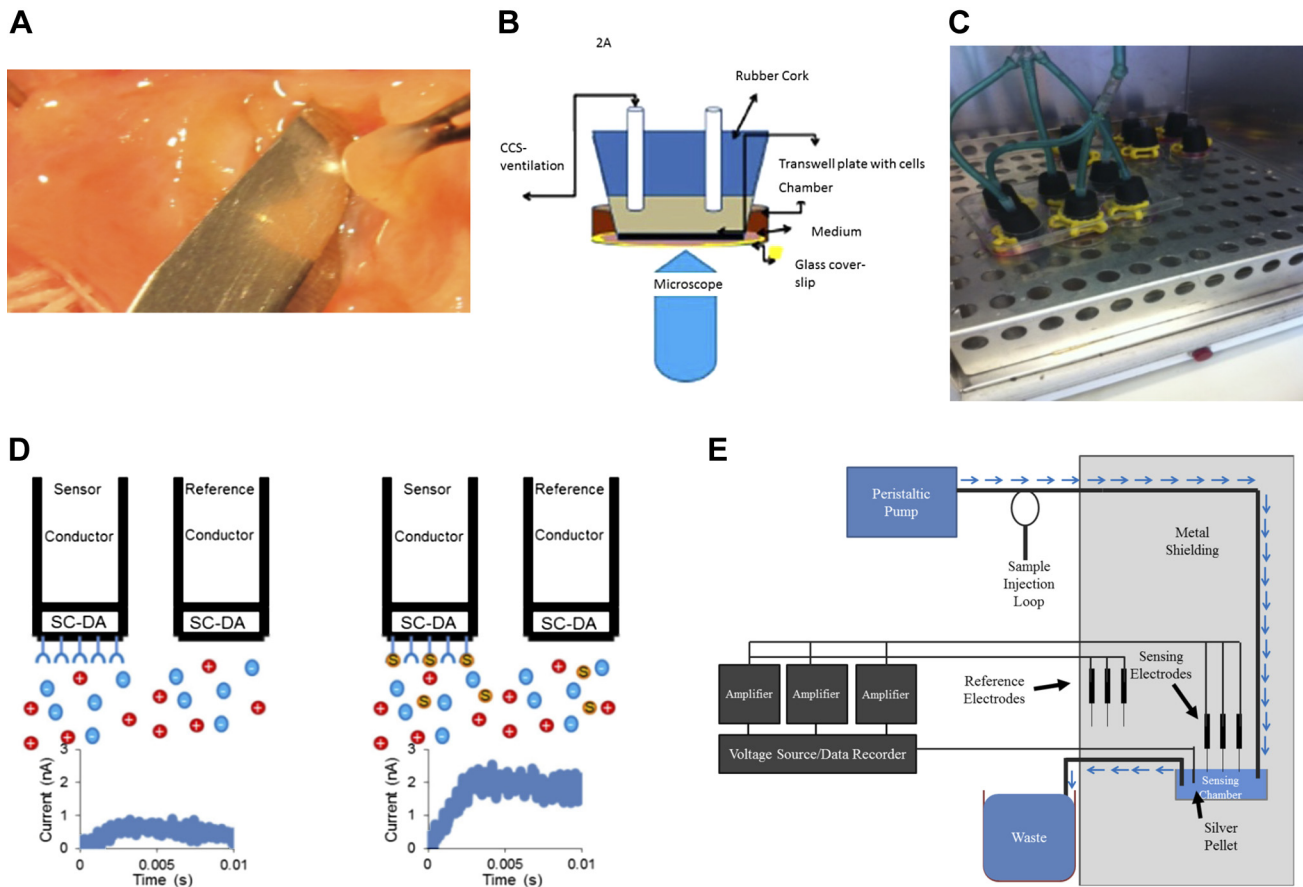
Fig. 1. Materials and methods. *A*: isolation of cells ex vivo from a human bronchus using a submucosal normal saline blister, followed by culture and growth on human fibronectin cellware slides. *B*: cultures loaded with fluo-3 AM underwent cyclic compressive stress (CCS) on the microscope stage using a syringe attached to the sealed chamber. Emission (493–582 nm; 15% power) was imaged on a Leica TCS-SP5 confocal microscope. *C*: CCS on intact wells of cultured, ciliated epithelial cells at air-liquid interface (ALI) was generated using a custom manifold sealed to each transwell (culture medium on the basolateral side) attached to a heated and humidified rodent ventilator in a 37°C, in 5% CO_2 incubator. Control cells (*right*) were treated the same way but not ventilated. *D*: schematic of the *S*-nitrosocysteine immunosensor experiments. This consists of a sensing and reference electrode, both of which are made up of a carbon fiber (Conductor) with a semiconducting polydopamine-coated tip (SC-DA; see also *E*, below). The SC-DA of the sensing electrode has been coated with anti-*S*-nitrosocysteine antibodies to provide selective binding. Under baseline conditions these electrodes show a flat charging curve (*left*), but when bound to an *S*-nitrosothiol (S), they produce an electrical signal. The assay does not detect glutathione or cysteine. Each sensor is freshly calibrated before each assay. *E*: circuit for the capacitance-based sensor system. Details of the sensor system, used both for the antibody-based (see *D*) and the chemosensor *S*-nitrosothiol assays are described in detail in Ref. 53. After dilution, the sample (pretreated with formaldehyde in the case of the chemosensor experiments) enters a custom Faraday cage at a fixed rate and is exposed to polydopamine-tipped carbon filament sensing electrodes [coated with anti-*S*-nitrosocysteine (CSNO) antibody in the case of the antibody-based experiments] with pulsed voltage (Dagan, Minneapolis, MN; SR560 preamplifiers from Stanford Research, Sunnydale, CA). Change in pulse current relative to untreated reference electrodes is recorded and compared with standards of *S*-nitrosoglutathione and CSNO.

the nucleus. Using this feature as opposed to the standard bright-field option allowed for a much tighter separation of clustered cells. All further analysis was then carried out on single cells. To identify representative intact cells, the size of the nucleus was tested for overlapping colocalization with CFTR. Cells that showed low colocalization of CFTR with DRAQ5 were then evaluated by the total area of the nucleus, allowing separation of viable intact cells from dead or apoptotic cells. Using this separation method yielded typically about ~10% of cells useful for analysis per sample.

ImageJ Area Under the Curve Calculations

Images of cells were exported from IDEAS and analyzed using the Plot Profile option of ImageJ. For each cell, the area under the curve for the CFTR signal was calculated using GraphPad Prism. Statistical significance analysis was carried out in GraphPad Prism (Tukey method to flag outliers, nonparametric two-tailed Mann-Whitney).

Calcium Flux Experiments

The bottom of a microdish chamber (Ibidi, Munich, Germany) was replaced with a glass coverslip. A rubber stopper in the transwell was attached to a manually operated piston for CCS with air injections at a rate of ~1/min, each injection lasting ~20 s (see Fig. 1*B*). Cells were incubated with 50 µl/well of 12 mM fluo 3-acetoxymethyl ester (FAM; Life Technologies; in air with 5% CO_2; 37°C; 30 min) and imaged with an inverted microscope DMI6000 integrated to a Leica TCS-SPX confocal workstation with a ×20 N.A. 0.7 objective lens. Images were collected with ×3 digital zoom. To minimize focal drift, the stage and imaging chamber were equilibrated for 60 min before the experiment, the laser dwell time per pixel was increased to ~1,000 Hz with bidirectional mode scanning, and the pinhole was set at 1.5 Airy units. An argon laser of 488-nm line at 15% power was used to excite the cells loaded with fluo 3-AM, and fluorescence emission was recorded in the range of 493–582 nm with ~40% quantum efficiency

PMT (hybrid detector) set at 75 V. Imaging was done in "xyt" mode using time series, and images were recorded at every 5 s up to 7 min and 40 s. Data from 33 different regions of interest were monitored to study the Ca^{2+} flux.

Human Fasting Exhaled NO Measurements: In Vivo CCS

The fraction of exhaled NO (F_{ENO}) was measured using the Aerocrine MINO (Stockholm, Sweden) according to the manufacturer's instructions immediately before and immediately after treatment in the airway clearance vest (Hill Rom, Chicago, IL; frequency: 10 Hz; pressure: 10 cm water; 10 min). Subjects were nonsmoking volunteers, 20–60 yr old, with no pulmonary disease. Assays were performed in the morning after an overnight fast to prevent both *1*) gastric nitrite conversion to NO (40, 59), possibly compressed from the stomach into the exhaled air by the vest; and *2*) an airway-reducing environment that would deplete NOx (40).

Immunoblots

Cell lysates were run on a 4–15% SDS-page gel, and the membrane was incubated overnight with primary antibody. For human CFTR blots, we used anti-CFTR MAB25031 (2060; R&D Systems SC; 1:500), with secondary (SC-2061; Santa Cruz Biotechnology; 1:3,000). For murine CFTR blots, we used anti-CFTR NB300-511 (Novus; 1:1,000) and secondary SC-2973 (1:3,000). For anti-β-actin we used 13E5 (Cell Signaling; 1:2,000) and secondary was SC-2054 (Santa Cruz Biotechnology; 1:3,000). For nNOS, the primary was ab76067 (Abcam; 1:500) and secondary was SC-2054 (Santa Cruz Biotechnology; 1:3,000). For iNOS, the primary was ab3523 (Abcam; 1:500) and secondary was SC-2054 (Santa Cruz Biotechnology; 1:3,000). For phospho-eNOS, the primary AB (pS 1177) was from BD Transduction Laboratories (1:1,000) and secondary was SC-2060 (Santa Cruz Biotechnology; 1:3,000). For GSNO reductase (GSNOR; ADH5), the primary was 11051-1-AP (Proteintech; 1:1,000) and secondary was SC2054 (Santa Cruz Biotechnology; 1:3,000). Blots were visualized using the Biorad Chemidoc System.

S-Nitrosothiol Assays

S-nitrosothiols were measured by three complementary methods. Anaerobic reduction/chemiluminescence was performed on whole cell lysates as previously described (15). A novel method was used for measuring *S*-nitrosothiols in small, apical volumes using a polydopamine-coated carbon fiber electrode (Fig. 1*D*; CFE-2; ALA Scientific) reacted with either monoclonal anti-*S*-nitrosocysteine (Creative Dynamics; sensing electrode) or buffer (reference electrode) as previously described using other antibodies (49, 50). Baseline measurements (sensing and reference electrodes in 10 mM Tris, pH 7.5, running buffer) used a 0.2-s current injection by means of a ±50-mV step potential (ITC-1600; HEKA) with a Ag/AgCl₂ ground pellet. The baseline measurement was repeated (twice, adding fresh running buffer), and the current responses of the sensing and reference electrodes were recorded in fresh buffer to ensure a stable baseline. Standard *S*-nitrosothiol solutions (24) or airway cell apical medium samples were then added to the running buffer. The maximum difference in current response by the sensing and reference electrode after baseline subtraction was recorded (49, 50). This method was adapted as a chemical detection system for low concentrations of *S*-nitrosothiols [see Supplemental Data: https:/doi.org/10.17605/OSF.IO/S6G24) (23, 31)].

Murine Studies

Immunoblot studies of eNOS $^{-/-}$ *mice.* eNOS$^{-/-}$ and background (C57Bl6) lungs were isolated as described previously (59). Tissue was homogenized in CFTR lysis buffer [100 mM NaCl, 50 mM NaF, 50 mM Tris·HCl, pH 7.5, 1% NP-40, 0.25% sodium deoxycholate, 1 mM EDTA, 1 mM EGTA, and protease inhibitor cocktail set III (Calbiochem)] and immunoblotted for CFTR as described above.

Study approvals. Animal use protocols were approved by the Institutional Animal Care and Use Committee at Case Western Reserve University (CWRU). Each of the clinical elements of the study [primary cell culture (PCC), ex vivo epithelial preparation (EVEP), and F_{ENO}/airway clearance vest (FAV) studies] was reviewed and approved by the Rainbow Babies and Children's Hospital (PCC, FAV), University of Virginia (PCC and EVEP), and/or UNC, Chapel Hill (PCC) Institutional Review Boards, and subjects signed informed consent before participating.

Statistical Analysis

Pairwise comparisons were analyzed by *t*-test if normally distributed with equal variance and rank-sum testing if not. Paired *t*-test was used for pair-wise comparisons. Multiple comparisons were similarly analyzed either by ANOVA or ANOVA on ranks following Dunn's test. Data are expressed as means ± SE or median ± interquartile range (IQR), as appropriate. $P < 0.05$ was considered significant.

RESULTS

Endothelial NOS Is Present in Human Airway Epithelial Cells In Vitro and Ex Vivo

We used human ALI cultured cells from five normal subjects and four F508Del homozygous cells listed in Table 1 and annotated throughout as "ALIx." We confirmed previous work (33) showing that iNOS is minimally expressed in F508Del homozygous cultures (*n* = 3 each; Fig. 2*A*; human primary ALI cultures, F508/F508, from Charles River and UNC; Table 1, ALI 1 and 2) and showed that nNOS was also essentially not detectable (Fig. 2*A*). However, eNOS was present and was phosphorylated at serine 1177, thus capable of activation by calcium flux and calmodulin binding (38) (*n* = 3; Fig. 2, *A* and *B*; human primary ALI cultures, F508/F508, from Charles River and UNC; Table1: ALI 1 and 2). Expression of phospho-eNOS was greater than that of nNOS and iNOS (*P* < 0.001; Fig. 2*B*). Controls were WT murine lung homogenate (eNOS), WT murine brain homogenate (nNOS), and the macrophage cell line RAW 264.7 (iNOS) as shown in Fig. 2*A*. Consistent with previous reports (64, 67), eNOS expression was apical in situ in airway epithelium of operative lobectomy specimens from humans with lung cancer (41) (Fig. 2*C*; *n* = 3 subjects). It was also apical in WT human pseudostratified epithelium grown at ALI (Fig. 2*D*; human primary ALI cultures, WT, from UNC; Table1: ALI 5). In F508Del homozygous preparations, it was apical and partially colocalized with dynein (Fig. 2*E*; *n* = 4, human primary ALI cultures, F508/F508, from UNC; Table1: ALI 2).

Cyclic Compression Leads to Cyclic Fluxes of Calcium into Human Airway Epithelial Cells

Because eNOS is activated by Ca^{2+}-calmodulin binding (25), we next confirmed that pulses of CCS resulted in cyclic Ca^{2+} flux into pseudostratified epithelial cells (1, 39). Each pulse resulted in an influx of calcium (Fig. 3, *A* and *B*; *n* = 16 cells/experiment, human primary ALI cultures, WT, from UNC; Table1: ALI 5). However, we did not find eNOS activation in unciliated mononoloyer airway epithelia cells in culture (CFBE41o⁻). We treated the CFBE cells with calcium ionophore A23187 with 5 μM Ca ionophore for 2 min and measured cellular nitrite levels (3). There was no change
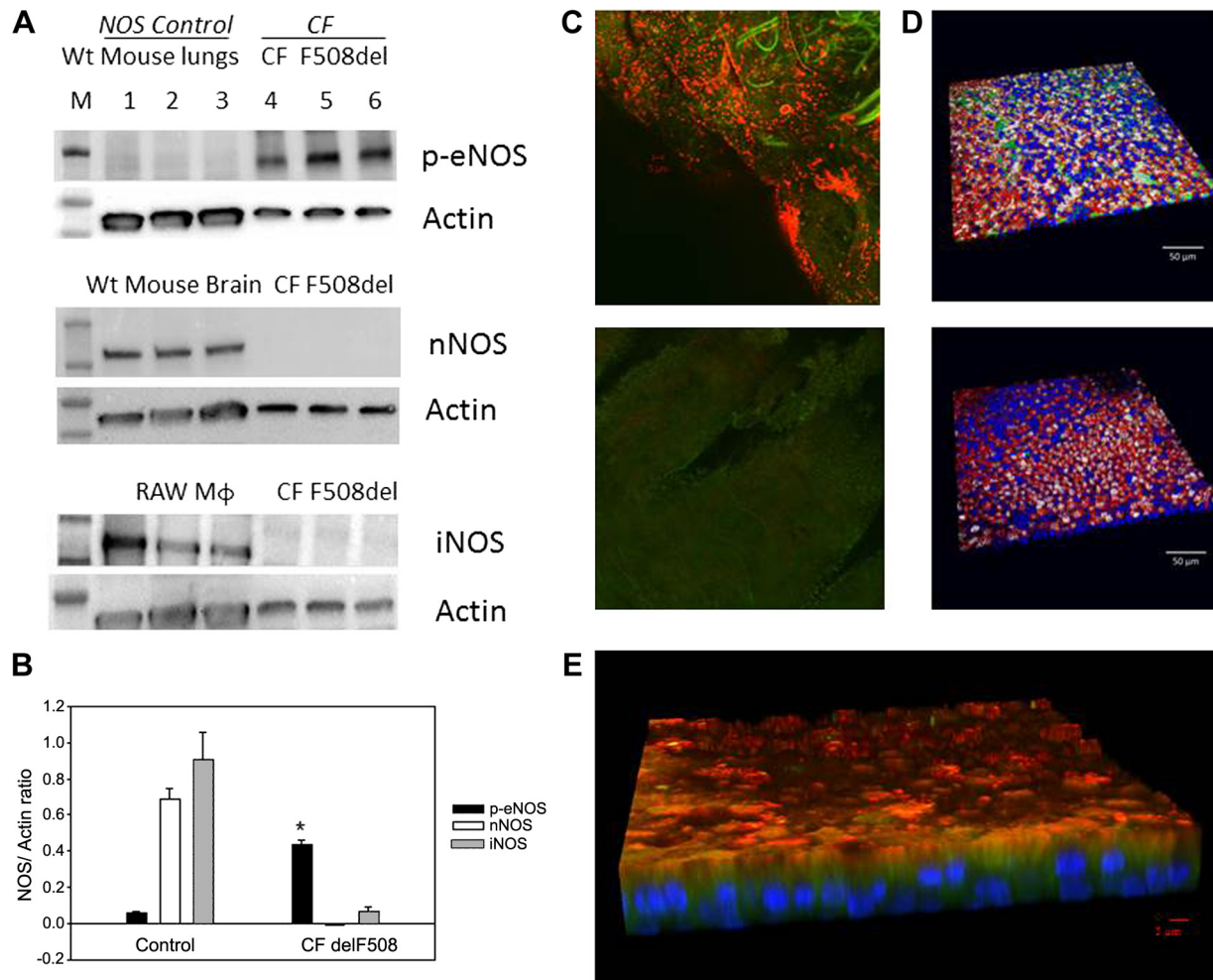
Fig. 2. Endothelial nitric oxide synthase (eNOS) expression in human airway pseudostratified epithelium. *A* and *B*: ciliated air-liquid interface (ALI) culture membranes from an F508Del cystic fibrosis (CF) transmembrane regulator (CFTR) homozygous patient (2 filters/lane) and wild-type (WT) mouse lungs' tissue were immunoblotted for phospho-eNOS S1177 (*top*). In a separate experiment, membranes from an F508Del CFTR homozygous patient and WT mouse brain' tissue were immunoblotted for neural nitric oxide synthase (nNOS; *middle*) and inducible nitric oxide synthase (iNOS; *bottom*). RAW cells macrophages served as a control for iNOS. Each membrane was stripped and re-probed for β actin (ALI 1 and 2). *B*: phospho-eNOS immunostaining was greater than for iNOS and nNOS in CF F508Del (*$P < 0.001$). *C*: eNOS staining from an ex vivo epithelial prep from *A* underwent immunofluorescent staining. *C*, *top*: eNOS (red) and dynein (green) are apical. *C*, *bottom*: negative control image shows no autofluorescence (ALI 7). *D*: ciliated ALI cultures from a non-CF subject (ALI 5) were immunostained for eNOS (*top*, green) or isotype control (*bottom*). Background was stained for filamentous actin (red), ciliary tubulin (white) and nuclei (blue). Sparse apical eNOS is observed. *E*: ciliated ALI cultures from a F508Del homozygous patient (ALI 2) were immunostained for eNOS (red), which is near apical and at times colocalized with dynein (green). Note sparse apical staining and absence of colocalization with the nucleus (DAPI; blue) or basal cells.

$(47.2 \pm 18 \ \mu M$ pre; $67.1 \pm 9.8 \ \mu M$ post; $n = 3$ each; $P =$ NS), suggesting that eNOS was not activated by calcium flux in the absence of cilia, likely because there is very little present in unciliated airway epithelial cells in culture (3).

Cyclic Compression Leads to Nitrogen Oxide Production by Human Airway Epithelial Cells

To determine whether CCS-induced calcium flux could activate eNOS, we measured epithelial NOS-derived *S*-nitrosothiols, chosen because of their potential roles in CFTR maturation (28, 42, 65, 66), before and after CCS (Fig. 3, *B–E*; human primary ALI cultures, F508/F508, from Charles River; Table1: ALI 1 and 2). The CCS ΔP was 15 cm of water, not as extreme as predicted during an asthma exacerbation, but substantially higher than in quiet breathing (48). *S*-nitrosothiol levels in the airways are near the limit of detection using traditional assays (23, 24, 65), particularly in CF (26). We

therefore employed a recently developed class of capacitance-based *S*-nitrosothiol assay with nM sensitivity (31, 53, 55) (Fig. 1*E*) in addition to traditional reduction/chemiluminesce. All assays were performed by investigators blind to the CCS treatment status. In all, we studied 61 filters from three CF subjects. All assays showed that CCS increased epithelial *S*-nitrosothiol levels in CF pseudostratified airway epithelial cells harvested immediately after CCS. First, by reduction/chemiluminescence, whole cell *S*-nitrosothiol levels increased from 0.015 (IQR 0.0025–0.028) pmol/μg protein (control; $n = 8$) to 0.06 (IQR 0.04–0.145) pmol/μg protein (CCS; $n = 9$; $P = 0.002$; Fig. 3*C*; Table 1: ALI 2). Second, we used the capacitance-based immunosensor (31, 55) coupled with an anti-*S*-nitrosocysteine (CSNO) antibody (59) to measure the apical *S*-nitrosothiol signal (sensor placed in fluid from the apex, adjacent to the eNOS localization; Fig. 3*B*). This signal increased after CCS from 1 (IQR 0–2) nAmp (control; $n = 3$)
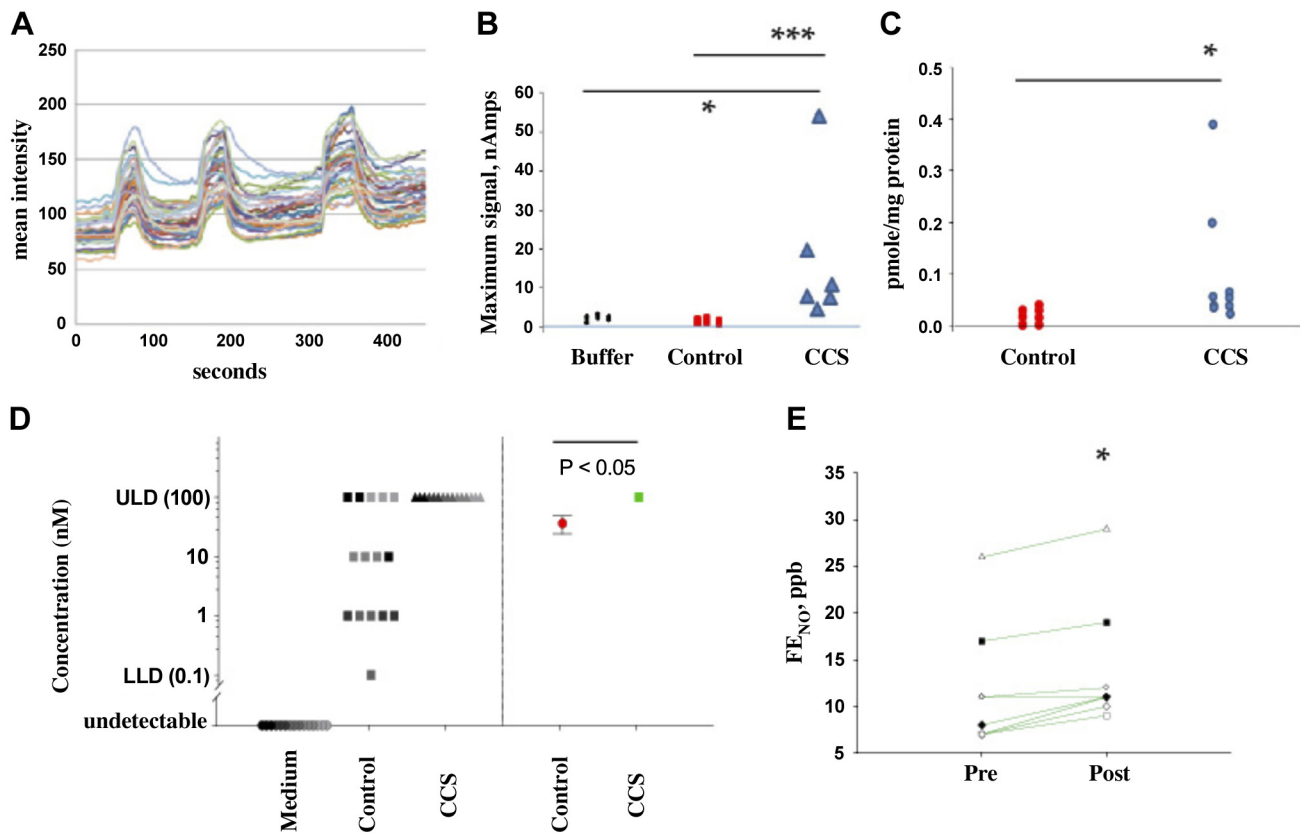
Fig. 3. Cyclic compressive stress (CCS) increases apical Ca^{2+} flux and nitrogen oxide formation in human airway epithelial cells at air-liquid interface (ALI). *A*: Ca^{2+} influx into the apex of these cells ($n = 16$; ALI 5) with each pulse of CCS (blue arrows). This experiment was repeated 3 times. *B*: sensor response from the system shown in Fig. 1*D* in apical medium measured after CCS from cystic fibrosis (CF), ciliated cells at ALI untreated ($n = 3$) or treated with CCS as shown in 1C ($n = 6$; ALI 3). The *S*-nitrosothiol signal was higher after CCS. *$P < 0.05$, CCS vs. buffer; ***$P < 0.05$, CCS-treated vs. control cells. *C*: after CCS, F508Del homozygous cells were snap frozen in liquid nitrogen. Blinded reduction-chemiluminescence assay showed *S*-nitrosothiol content/protein after CCS ($n = 9$) was greater than control ($n = 8$; *$P = 0.002$; ALI 1 and 2). *D*: assays were also performed on a fresh set of cells using a modified sensor as described in Ref. 53. *Left* dots represent the individual signals from each set of cells (using the log scale with which the measurements were made), while the *right* dots represent the geometric mean of the results at *left* (red: control with standard error; green: cells received CCS). Because this sensor acts as an on/off toggle for the presence or absence of *S*-nitrosocysteine, we performed serial dilutions of the cell lysate and medium over 4 logs (0.01–100 nM). All cells had *S*-nitrosothiols [36 ± 12 nM; greater than medium alone (0 ± 0 nM), $n = 5$ samples, 3 replicates each; $P < 0.001$]. CCS increased *S*-nitrosothiol levels to the point that the sensor was saturated (≥ 100 nM in all samples, $n = 5$ samples, 3 replicates each, $P < 0.001$ compared with untreated; ALI 8). *E*: normal subjects were studied after an overnight fast for fraction of exhaled NO (F_{ENO}) analysis before and after airway clearance vest treatment: 10 Hz, 10 cm water, 10 min; $n = 8$). F_{ENO} consistently increased in these subjects with in vivo CCS (*$P = 0.006$ by paired *t*-test). ULD, upper limit of detection; LLD, lower limit of detection.

to 10.5 (IQR 8–20) nAmp ($P < 0.05$; $n = 6$; Fig. 3*B*; ALI 3). Finally, we used this capacitance-based sensor system with formaldehyde pretreatment as recently described and standardized (53) (Fig. 1*E*) to measure whole cell lysate *S*-nitrosothiols. Each assay in Fig. 3*D* was performed on a fresh set of cells using a sensor (53) that acts as acts as an on/off toggle for the presence or absence of CSNO. We therefore performed serial dilutions of the cell lysate over four logs on WT primary airway epithelial cells) with cyclic compressive stress (labeled as "CCS") and without CCS (labeled as "control") and medium alone (collected from these cells). The difference between the Fig. 3*D, left*, and Fig. 3*D, right*, is that Fig. 3*D, left*, dots represent the individual signals from each set of cells (using the log scale with which the measurements were made), while Fig. 3*D, right*, is the geometric mean of the Fig. 3*D, left*, results (red: control with standard error; green: cells that received CCS). There is a significant difference in these geometric mean CSNO levels between WT cells at baseline and those and receiving CCS ($P \leq 0.05$). This method confirmed that all cells had *S*-nitrosothiols [36 ± 12 nM; greater than medium alone

(0 ± 0 nM), $n = 5$ samples, 3 replicates each; $P < 0.001$]. CCS increased *S*-nitrosothiol levels to the point that the sensor was saturated (≥ 100 nM in all samples, $n = 5$ samples, 3 replicates each, $P < 0.001$ compared with untreated; human primary ALI cultures, F508/F508, from CWRU; Table 1: ALI 8; Fig. 3*D*). Finally, to confirm that the increase of *S*-nitrosothiol level associated with CCS was caused by increased production, rather than decreased catabolism (41), we measured the effect of CCS on GSNO reductase expression in human primary ALI cultures (F508/F508 from Charles River; Table 1: ALI 3). We have found no difference in GSNOR expression and activity following CCS treatment (densitometry = 0.80 ± 0.43, vs. control 0.55 ± 0.53; $n = 3$ each; $P = $ NS).

Measurement of airway *S*-nitrosothiols in vivo before and after CCS would require pre- and post-CCS bronchoscopy. To avoid this invasive procedure, we studied fraction of exhaled NO (F_{ENO}), a marker for airway GSNO (57): airway GSNO can be labile but increasing GSNO airway increases F_{ENO} because of homolytic GSNO cleavage to form NO (40, 57). Thus a small change in F_{ENO} can be a marker for GSNO

formation downstream of eNOS activation. However, the determinants of F_{ENO} are complex (12, 21, 40, 51, 57) and eNOS can activate counterregulatory GSNO reductase (5), which, in an NADH-dependent fashion, gradually decreases GSNO (38). Feeding increases cellular NADH (63), which increases GSNOR activity (38, 61). Therefore, we studied F_{ENO} in human subjects after an overnight fast. Measurements were made before and after in vivo airway clearance vest treatment, which cyclically increases pressure and shear stress across the ALI in vivo. The airway clearance system consistently increased fasting F_{ENO} in humans in vivo from 12.7 to 14.8 ppb ($n = 8$; $P = 0.006$; Fig. 3E). Since it does not do so in the fed state (56), these in vivo data are consistent with the observation that CCS leads to S-nitrosothiol formation in vitro.

Cyclic Compression Leads to Increased F508Del CFTR Maturation in Human Airway Epithelial Cells in a Cilia-Dependent Fashion

Single cell flow-based Imagestream analysis of cells grown in ALI cultures using area under the curve (AUC) calculation of total CFTR density (Fig. 4; Supplemental Figures S1, S2, and S3; see Supplemental Data: https:/doi.org/10.17605/ OSF.IO/S6G24) showed very little CFTR staining in the isotype control and weak intracellular staining in F508del homozygous cells. However, there was strong, apical expression in healthy, control cells and in F508Del CFTR homozygous cells treated with either CCS or 30°C. Specifically, filters of ALI cultures were placed in our custom CCS manifold (as described above) at 37°C, 5% CO_2 as above for 30 min, 2 h, or 3 h (Fig. 4C). Control F508 Del homozygous ALI cultures were placed into a 30°C/5% CO_2 incubator overnight (positive control) or in the CCS incubator (37°C; negative control). Non-CF ALI cultures (37°C) were used as an additional control. Assessment and quantification of CFTR were performed using imaging flow cytometry with RB7865, a polyclonal antibody directed toward the ECL-1 loop of CFTR (43), for eNOS and DRAQ5 for nuclear DNA. Without CCS treatment the F508Del CFTR localization was minimal, and diffuse in the cell. For an in-depth analysis cells were selected and cross sectionally assessed as indicated in the Supplemental Fig. S3 (see Supplemental Data: https:/doi.org/10.17605/OSF.IO/ S6G24). An example of cells of each population is given with the corresponding profile next to each cell. The green line shows the distribution of CFTR along the longitudinal cut of the cells. Importantly, WT cells stained with the prebleed serum of rabbit RB7865 showed very little CFTR stain (isotype control), while the immune serum showed a very clear signal on the same batch of cells. In all cases we observed a significant difference when treating cells with CCS. The CFTR intensity was proportional to the area under the curve. By contrast, CCS did not change eNOS expression (see Supplemental Fig. S4; https:/doi.org/10.17605/OSF.IO/S6G24).

Immunoblot assays confirmed that expression of F508Del CFTR was increased by CCS in ciliated pseudostratified cultures (Fig. 5A; human primary ALI cultures, F508/F508, from Charles River; Table1: ALI 1). Specifically, partially mature CFTR (B band) increased relative to β-actin (from 0.10 ± 0.02 to 0.46 ± 0.1; $n = 9$ lanes, 2 wells/lane; $P < 0.001$), and the fully mature CFTR (C band) increased from 0.12 ± 0.03 relative to β-actin to 0.42 ± 0.02; $n = 9$ lanes; $P < 0.001$; (Fig.

5B; human primary ALI cultures, F508/F508, from Charles River and UNC (Table1: ALI 1 and 2). On the other hand, CCS did not result in any change F508Del CFTR expression in nonciliated, monolayer CF epithelial cell lines (CFBE41o⁻; $n = 3$ lanes; 6 wells; $P = NS$; Fig. 5C), consistent with the lack of eNOS activation using calcium ionophore in these cells (above). If anything, there was a tendency for the B band to decrease with CCS in the absence of cilia. CCS also did not significantly affect WT CFTR maturation in WT CFBE41o⁻ cells ($n = 3$; Fig. 5D), again suggesting an essential role for cilia.

Increased F508Del CFTR Maturation in Human Airway Epithelial Cells Exposed to Cyclic Stress Is Dependent on TRPV4 and eNOS

We next studied the role of TRPV4-dependent Ca^{2+} flux (1, 39) and of NOS on the CCS effect to increase F508Del CFTR maturation (Fig. 5, E and F). Note that these cells express TRPV4 mRNA from early passage (S. H. Randell, unpublished observations) consistent with previous publications regarding TRPV4 protein expression (1, 39). CCS-induced CFTR maturation was inhibited by the TRPV4 inhibitor HC067047 (500 nM, 2 h, ($n = 4$ lanes, 8 wells each; $P < 0.01$; Fig. 5E; human primary ALI cultures, F508/F508, from UNC; Table1: ALI 2). Furthermore, CCS-induced WT CFTR maturation was inhibited by the NOS inhibitor L-NAME (10 mM, 2 h; $n = 9$ lanes each; $P < 0.01$; Fig. 5F; human primary ALI cultures, WT, from CWRU and UNC; Table1: ALI 5 and 6), which inhibited S-nitrosothiol production from 3.3 ± 0.7 to 1.8 ± 0.1 nM; $n = 3$ each; $P < 0.05$; Fig. 5F, inset; human primary ALI cultures, WT, from UNC; Table1: ALI 5). Both B- and C-band CFTR, while present, were attenuated in eNOS⁻/⁻ mouse lung homogenates ($n = 3$ each; Fig. 5G). CCS in vitro decreased transepithelial resistance in Ussing chambers, likely because of disrupted cell junctions, precluding using this measure of CFTR function.

DISCUSSION

It is increasingly appreciated that cyclic changes in air pressure and flow affect the biology of ciliated airway epithelial cells in culture (6, 60), just as fluid flow alters endothelial cell biology (17). Here, we have studied the effect of changes in apical air pressure on human airway epithelial CFTR maturation. We report that cyclic compression, at least in part through TRPV4 and NOS, leads to increased CFTR expression in ciliated airway epithelial cultures.

Airway epithelial cilia have motor and sensory functions (14, 30, 36, 54). Sensory functions are both chemosensory and mechanosensory. Recent evidence suggests that ciliary chemosensory functions involve NOx (32). Here, we provide evidence that airway mechanosensory functions also involve NOx. This observation is consistent with previous data regarding olfactory cilia, in which eNOS is activated by calcium flux to signal olfaction (13). These data suggest a novel role for eNOS in the sensory functions of airway cilia.

Modification of trafficking proteins in the CFTR interactome by GSNO augments CFTR maturation, preventing CFTR degradation at the endoplasmic reticulum and plasma membrane (2, 42, 66). Exogenous GSNO increases F508Del CFTR maturation primarily by targeting the Hsp70/Hsp90 organizing
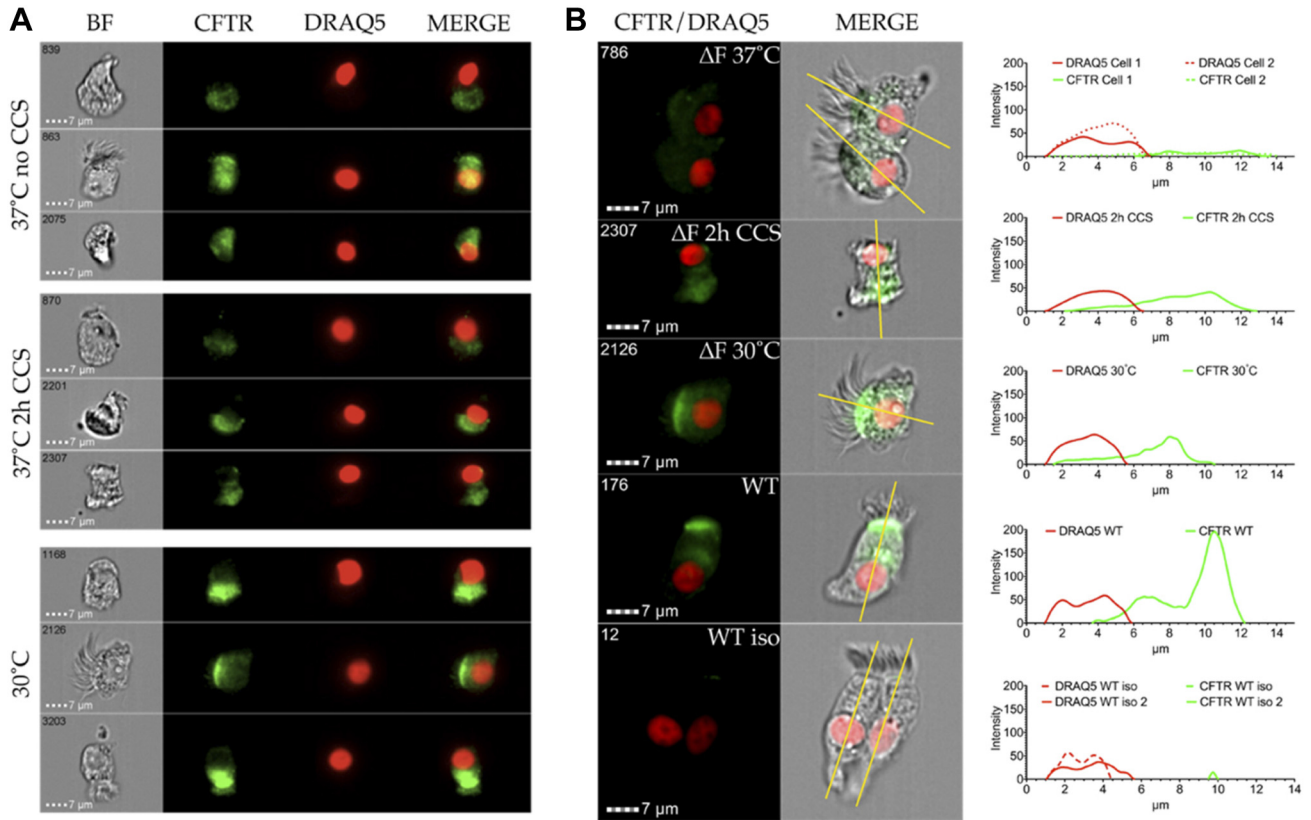
Fig. 4. Imaging flow cytometry analysis of human bronchial epithelial cells stained with anti- CFTR and DRAQ5. *A*: representative cells showing the localization of CFTR and DRAQ5 for nuclear stain. *B*: single cell analysis using ImageJ for profile analysis. The yellow line represents the section of the profile. The size of the nucleus is ~5 μm size (red). The histogram plot shows the nuclear and CFTR stain. Very little CFTR stain is observed in the isotype control (prebleed). *C*: area under the curve (AUC) analysis of the CFTR signal under different treatment conditions. CCS, cyclic compressive stress; WT, wild type. Outliers are indicated in magenta, the mean value is shown as +, and whiskers are calculated by Tukey method. *P* values were calculated by two-tailed nonparametric Mann-Whitney with 95% confidence level.

protein (Hop) for degradation, preventing Hop-CFTR interaction and, thereby, preventing CFTR degradation (42). Other mechanisms are relevant as well (41, 65), but epithelial siRNA experiments suggest that the Hop-dependent mechanisms is foremost.

However, GSNOR inhibition only improves weight gain, not lung function, in CF patients in vivo, consistent with evidence that GSNO production is decreased in the CF airway epithelium (33): inhibiting a catabolic enzyme is ineffective if there is little substrate. GSNO and other *S*-nitrosothiols are classically produced by NOS isoforms (16, 22, 25, 52, 58, 61). Neither nNOS nor iNOS are expressed significantly in CF airway epithelial cells (26) (Fig. 2). Our current data suggest that CCS-driven eNOS activation may help augment GSNO
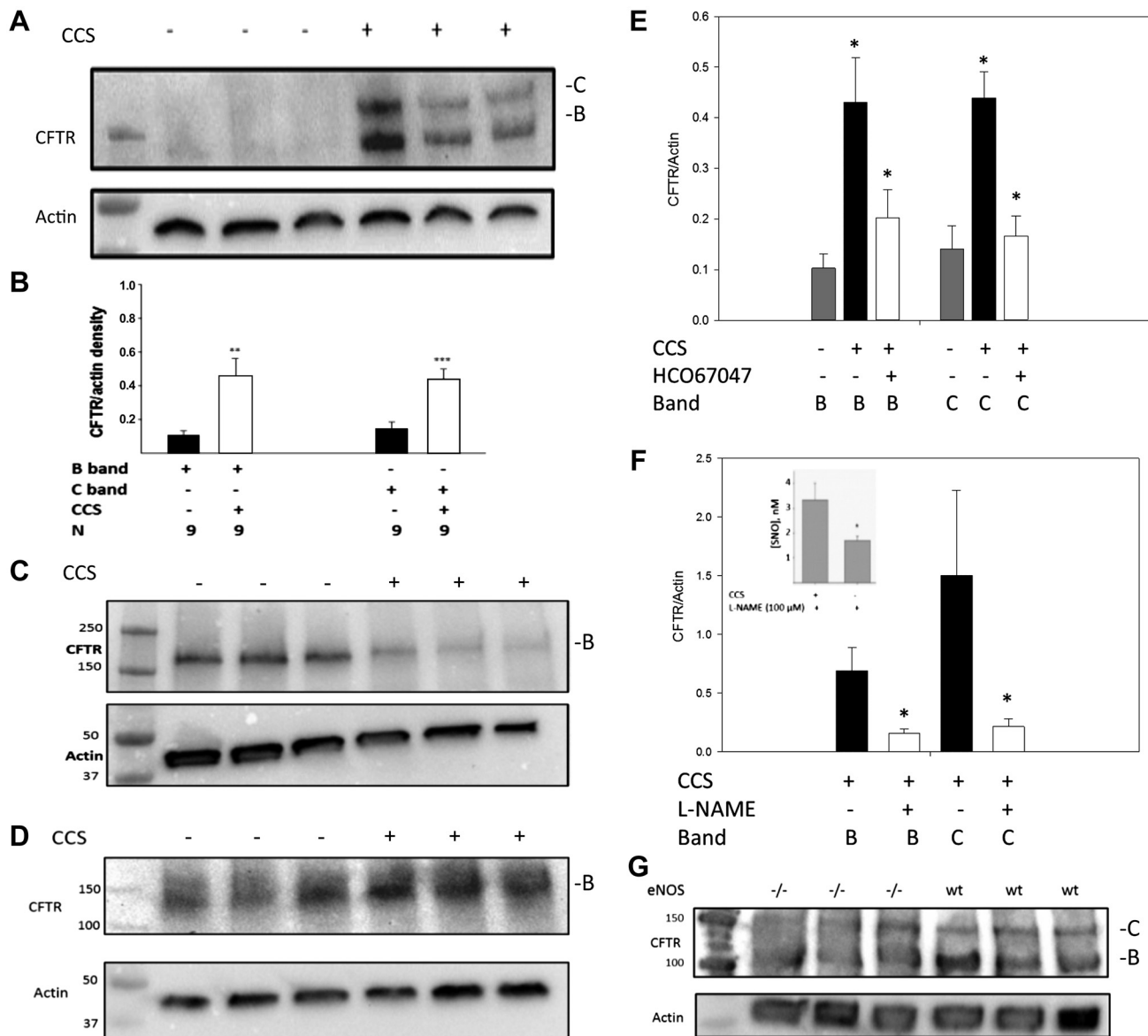
Fig. 5. Cyclic compressive stress (CCS) increases CFTR maturation in human airway epithelial cells, an effect requiring cilia, transient receptor potential vanilloid (TRPV4), and nitric oxide synthase (NOS). *A*: F508Del homozygous human airway cells [air-liquid interface 1 (ALI 1)] underwent CCS (see Fig. 2*C*) and immunoblotting for CFTR. CCS increased partially (B band) and fully (C band) mature CFTR. *B*: 9 replicates of experiment in *A* (ALI 1 and 2); **$P < 0.001$ by *t*-test and ***$P < 0.001$ (for nonparametric distribution) rank-sum test for B and C bands, respectively. *C* and *D*: nonciliated F508Del-transfected (*C*; CFBE41o$^-$) or wild-type (WT)-transfected CFBE41o$^-$ cells (*D*) studied as in *A*. CFTR did not change with CCS (P = NS), suggesting that cilia, not present in CFBE41o$^-$ cells, are required for the CCS effect. *E*: ciliated F508Del homozygous human airway cells (ALI 2) exposed as in *A–D* to CCS showed that the B and C bands increase (relative to actin) with CCS was inhibited by the TRPV4 inhibitor HC067047 [both *B* and *C* band, *$P < 0.01$, CCS vs control; CCS/H067047 did not differ from unventilated (P = NS); n = 4 each]. *F*: in WT ciliated airway epithelial cells (ALI 5 and 6), B and C bands increased with CCS, an effect partly blocked by nitro-L-arginine methyl ester [L-NAME; *$P < 0.01$, CCS vs control; CCS/L-NAME did not differ from unventilated (P = NS); n = 9]. *Inset*: *S*-nitrosothiols during CCS were decreased by L-NAME (n = 3 each; *$P < 0.05$). *G*: lungs from eNOS $^{-/-}$ mice expressed less B-band CFTR than those from WT. eNOS, endothelial nitric oxide synthase.

airway levels, and that increasing GSNO production, deficient in CF (26), may be more valuable for increasing CFTR maturation than inhibiting GSNO catabolism. Indeed, there may be little value to inhibiting GSNO catabolism if its substrate is deficient.

Genetic deletion of eNOS is associated with more methacholine responsiveness in a murine asthma model than is deletion of other NOS isoforms (11). However, eNOS produces low quantities of NO (ie, NO radical) relative to iNOS and is not frequently discussed in the context of airway NO production (51). This paradox is consistent with evidence that NO itself may be less important than is commonly supposed in human airway biology downstream of NOS activation (22, 40). For example, human airway smooth muscle is less responsive to endogenous levels NO than endogenous levels of GSNO (20); levels of NO in the airway are normally too low to be of any physiological relevance (23, 57); and eNOS activation causes location-dependent formation of *S*-nitrosothiols to signal local effects independent of the quantity of NO radical produced (25, 41). In this regard, eNOS activation to produce

GSNO in the airway epithelium could have many beneficial effects. *S*-nitrosothiols increase ciliary motility (37), relax airway smooth muscle (20, 22), and alter Na^+ and Cl^- currents (10, 29). Thus the pathway we describe here could help to explain certain benefits of airway pressure, like that in exercise. For example, positive pressure causes smooth muscle relaxation in precision-cut human lung slices (35). This involves an effect on the biophysical properties of airway smooth muscle but could also involve epithelial eNOS activation (22, 25). Because iNOS is minimally present in the CF epithelium and is not upregulated posttranslationally by calcium, our data suggest that it is eNOS, activated by CCS, that increases F508Del CFTR maturation. eNOS activity may be underappreciated in static cultures of airway epithelium.

Airway *S*-nitrosothiols were not measured directly in vivo. We used change in fasting F_{ENO} as a surrogate to avoid pre- and post-CCS bronchoscopy. In CF patients, F_{ENO} increases with increased airway GSNO in vivo (57). Note, however, that determinants of F_{ENO} are complex (46) and affected by airway pH, the airway microbiome, airway ADMA and arginine metabolism, and airway GSNOR activity (12, 21, 40, 51, 57). GSNOR activity is regulated by NADH availability, which is decreased in fasting (26, 38): CCS increases F_{ENO} in fasted subjects, whereas it does not in fed subjects (56). Thus these in vivo observations are supportive of the in vitro evidence for an increase in airway epithelial GSNO formation resulting from CCS. GSNO formation could be enhanced by use of GSNOR inhibitor, because the *S*-nitrosothiol compounds are labile (41), but we have focused here purely on formation. A range of airway clearance techniques and devices provide in vivo CCS for CF patients. Our findings could ultimately help provide markers to determine which clinical techniques would be most beneficial and which would not (44).

In summary, human airway epithelial cells respond to cyclic increases in airway pressure with an increase in CFTR expression. Consistent with previous publications (1, 39, 64, 67), this effect on CFTR likely involves Ca^{2+} flux into the cells to activate apical eNOS. CCS increases *S*-nitrosothiol formation and increases F508Del maturation in a TRPV4- and NOS-dependent fashion. Moreover, nonciliated airway epithelial cells fail to increase F508Del CFTR maturation in response to CCS. Taken together, these data suggest the possibility that approaches to increase cyclic airway compression, whether through airway clearance techniques or vigorous exercise itself, could benefit CF patients not only by mobilizing secretions, but also by correcting CFTR expression.

DISCLOSURES

No conflicts of interest, financial or otherwise, are declared by the authors.

AUTHOR CONTRIBUTIONS

B.G. conceived and designed research; N.M., J.B., C.U.C., L.S., J.V.S., K.Z., S.R., A.P., H.G., G.A., M.D., D.R.J., R.S., and S.H.R. performed experiments; N.M., J.B., L.S., J.V.S., and B.G. analyzed data; N.M. and B.G. interpreted results of experiments; N.M. and J.B. prepared figures; N.M. drafted manuscript; B.G. edited and revised manuscript; B.G. approved final version of manuscript.

REFERENCES

1. **Alenmyr L, Uller L, Greiff L, Högestätt ED, Zygmunt PM.** TRPV4-mediated calcium influx and ciliary activity in human native airway epithelial cells. *Basic Clin Pharmacol Toxicol* 114: 210–216, 2014. doi:10.1111/bcpt.12135.

2. **Angers RC, Mutka SC, Bove, P, Gabriel SE.** Pharmacological correction and acute inhibition of GSNOR results in improved in vitro CFTR function. 2015 North American Cystic Fibrosis Conference. Phoenix, AZ.

3. **Asano K, Chee CB, Gaston B, Lilly CM, Gerard C, Drazen JM, Stamler JS.** Constitutive and inducible nitric oxide synthase gene expression, regulation, and activity in human lung epithelial cells. *Proc Natl Acad Sci USA* 91: 10089–10093, 1994. doi:10.1073/pnas.91.21.10089.

4. **Baraldi E.** Chronic respiratory diseases and sport in children. *Int J Sports Med* 21, *Suppl* 2: 103–104, 2000. doi:10.1055/s-2000-8499.

5. **Brown-Steinke K, deRonde K, Yemen S, Palmer LA.** Gender differences in S-nitrosoglutathione reductase activity in the lung. *PLoS One* 5: e14007, 2010. doi:10.1371/journal.pone.0014007.

6. **Button B, Boucher RC; University of North Carolina Virtual Lung Group.** Role of mechanical stress in regulating airway surface hydration and mucus clearance rates. *Respir Physiol Neurobiol* 163: 189–201, 2008. doi:10.1016/j.resp.2008.04.020.

7. **Button B, Cai LH, Ehre C, Kesimer M, Hill DB, Sheehan JK, Boucher RC, Rubinstein M.** A periciliary brush promotes the lung health by separating the mucus layer from airway epithelia. *Science* 337: 937–941, 2012. doi:10.1126/science.1223012.

8. **Button B, Okada SF, Frederick CB, Thelin WR, Boucher RC.** Mechanosensitive ATP release maintains proper mucus hydration of airways. *Sci Signal* 6: ra46, 2013. doi:10.1126/scisignal.2003755.

9. **Button B, Picher M, Boucher RC.** Differential effects of cyclic and constant stress on ATP release and mucociliary transport by human airway epithelia. *J Physiol* 580: 577–592, 2007. doi:10.1113/jphysiol.2006.126086.

10. **Chen L, Patel RP, Teng X, Bosworth CA, Lancaster JR, Matalon S.** Mechanisms of cystic fibrosis transmembrane conductance regulator activation by S-nitrosoglutathione. *J Biol Chem* 281: 9190–9199, 2006. doi:10.1074/jbc.M513231200.

11. **De Sanctis GT, MacLean JA, Hamada K, Mehta S, Scott JA, Jiao A, Yandava CN, Kobzik L, Wolyniec WW, Fabian AJ, Venugopal CS, Grasemann H, Huang PL, Drazen JM.** Contribution of nitric oxide synthases 1, 2, and 3 to airway hyperresponsiveness and inflammation in a murine model of asthma. *J Exp Med* 189: 1621–1630, 1999. doi:10.1084/jem.189.10.1621.

12. **Dweik RA, Comhair SA, Gaston B, Thunnissen FB, Farver C, Thomassen MJ, Kavuru M, Hammel J, Abu-Soud HM, Erzurum SC.** NO chemical events in the human airway during the immediate and late antigen-induced asthmatic response. *Proc Natl Acad Sci USA* 98: 2622–2627, 2001. doi:10.1073/pnas.051629498.

13. **Endo D, Yamamoto Y, Yamaguchi-Yamada M, Nakamuta N, Taniguchi K.** Localization of eNOS in the olfactory epithelium of the rat. *J Vet Med Sci* 73: 423–430, 2011. doi:10.1292/jvms.10-0353.

14. **Enuka Y, Hanukoglu I, Edelheit O, Vaknine H, Hanukoglu A.** Epithelial sodium channels (ENaC) are uniformly distributed on motile cilia in the oviduct and the respiratory airways. *Histochem Cell Biol* 137: 339–353, 2012. doi:10.1007/s00418-011-0904-1.

15. **Fang K, Ragsdale NV, Carey RM, MacDonald T, Gaston B.** Reductive assays for S-nitrosothiols: implications for measurements in biological systems. *Biochem Biophys Res Commun* 252: 535–540, 1998. doi:10.1006/bbrc.1998.9688.

16. **Foster MW, Hess DT, Stamler JS.** Protein S-nitrosylation in health and disease: a current perspective. *Trends Mol Med* 15: 391–404, 2009. doi:10.1016/j.molmed.2009.06.007.

17. **Frangos JA, Eskin SG, McIntire LV, Ives CL.** Flow effects on prostacyclin production by cultured human endothelial cells. *Science* 227: 1477–1479, 1985. doi:10.1126/science.3883488.

18. **Fulcher ML, Randell SH.** Human nasal and tracheo-bronchial respiratory epithelial cell culture. *Methods Mol Biol* 945: 109–121, 2012. doi:10.1007/978-1-62703-125-7_8.

19. **Galietta LJ, Lantero S, Gazzolo A, Sacco O, Romano L, Rossi GA, Zegarra-Moran O.** An improved method to obtain highly differentiated monolayers of human bronchial epithelial cells. *In Vitro Cell Dev Biol Anim* 34: 478–481, 1998. doi:10.1007/s11626-998-0081-2.

20. **Gaston B, Drazen JM, Jansen A, Sugarbaker DA, Loscalzo J, Richards W, Stamler JS.** Relaxation of human bronchial smooth muscle by S-nitrosothiols in vitro. *J Pharmacol Exp Ther* 268: 978–984, 1994.

21. **Gaston B, Kelly R, Urban P, Liu L, Henderson EM, Doctor A, Teague WG, Fitzpatrick A, Erzurum S, Hunt JF.** Buffering airway acid decreases exhaled nitric oxide in asthma. *J Allergy Clin Immunol* 118: 817–822, 2006. doi:10.1016/j.jaci.2006.06.040.

22. **Gaston B, Reilly J, Drazen JM, Fackler J, Ramdev P, Arnelle D, Mullins ME, Sugarbaker DJ, Chee C, Singel DJ.** Endogenous nitrogen oxides and bronchodilator S-nitrosothiols in human airways. *Proc Natl Acad Sci USA* 90: 10957–10961, 1993. doi:10.1073/pnas.90.23.10957.

23. **Gaston B, Singel D, Doctor A, Stamler JS.** S-nitrosothiol signaling in respiratory biology. *Am J Respir Crit Care Med* 173: 1186–1193, 2006. doi:10.1164/rccm.200510-1584PP.

24. **Gow A, Doctor A, Mannick J, Gaston B.** S-Nitrosothiol measurements in biological systems. *J Chromatogr B Analyt Technol Biomed Life Sci* 851: 140–151, 2007. doi:10.1016/j.jchromb.2007.01.052.

25. **Gow AJ, Chen Q, Hess DT, Day BJ, Ischiropoulos H, Stamler JS.** Basal and stimulated protein S-nitrosylation in multiple cell types and tissues. *J Biol Chem* 277: 9637–9640, 2002. doi:10.1074/jbc.C100746200.

26. **Grasemann H, Gaston B, Fang K, Paul K, Ratjen F.** Decreased levels of nitrosothiols in the lower airways of patients with cystic fibrosis and normal pulmonary function. *J Pediatr* 135: 770–772, 1999. doi:10.1016/S0022-3476(99)70101-0.

27. **Gunst SJ, Stropp JQ.** Pressure-volume and length-stress relationships in canine bronchi in vitro. *J Appl Physiol (1985)* 64: 2522–2531, 1988. doi:10.1152/jappl.1988.64.6.2522.

28. **Howard M, Fischer H, Roux J, Santos BC, Gullans SR, Yancey PH, Welch WJ.** Mammalian osmolytes and S-nitrosoglutathione promote delta F508 cystic fibrosis transmembrane conductance regulator (CFTR) protein maturation and function. *J Biol Chem* 278: 35159–35167, 2003. doi:10.1074/jbc.M301924200.

29. **Jain L, Chen XJ, Brown LA, Eaton DC.** Nitric oxide inhibits lung sodium transport through a cGMP-mediated inhibition of epithelial cation channels. *Am J Physiol Cell Lung Mol Physiol* 274: L475–L484, 1998. doi:10.1152/ajplung.1998.274.4.L475.

30. **Jain R, Javidan-Nejad C, Alexander-Brett J, Horani A, Cabellon MC, Walter MJ, Brody SL.** Sensory functions of motile cilia and implication for bronchiectasis. *Front Biosci (Schol Ed)* 4: 1088–1098, 2012.

31. **Jastrzebska MM, Stepień K, Wilczok J, Porebska-Budny M, Wilczok T.** Semiconductor properties of melanins prepared from catecholamines. *Gen Physiol Biophys* 9: 373–383, 1990.

32. **Jiao J, Wang H, Lou W, Jin S, Fan E, Li Y, Han D, Zhang L.** Regulation of ciliary beat frequency by the nitric oxide signaling pathway in mouse nasal and tracheal epithelial cells. *Exp Cell Res* 317: 2548–2553, 2011. doi:10.1016/j.yexcr.2011.07.007.

33. **Kelley TJ, Drumm ML.** Inducible nitric oxide synthase expression is reduced in cystic fibrosis murine and human airway epithelial cells. *J Clin Invest* 102: 1200–1207, 1998. doi:10.1172/JCI2357.

34. **Kobzik L, Bredt DS, Lowenstein CJ, Drazen J, Gaston B, Sugarbaker D, Stamler JS.** Nitric oxide synthase in human and rat lung: immunocytochemical and histochemical localization. *Am J Respir Cell Mol Biol* 9: 371–377, 1993. doi:10.1165/ajrcmb/9.4.371.

35. **Lavoie TL, Krishnan R, Siegel HR, Maston ED, Fredberg JJ, Solway J, Dowell ML.** Dilatation of the constricted human airway by tidal expansion of lung parenchyma. *Am J Respir Crit Care Med* 186: 225–232, 2012. doi:10.1164/rccm.201202-0368OC.

36. **Lee RJ, Cohen NA.** Bitter and sweet taste receptors in the respiratory epithelium in health and disease. *J Mol Med (Berl)* 92: 1235–1244, 2014. doi:10.1007/s00109-014-1222-6.

37. **Li D, Shirakami G, Zhan X, Johns RA.** Regulation of ciliary beat frequency by the nitric oxide-cyclic guanosine monophosphate signaling pathway in rat airway epithelial cells. *Am J Respir Cell Mol Biol* 23: 175–181, 2000. doi:10.1165/ajrcmb.23.2.4022.

38. **Liu L, Hausladen A, Zeng M, Que L, Heitman J, Stamler JS.** A metabolic enzyme for S-nitrosothiol conserved from bacteria to humans. *Nature* 410: 490–494, 2001. doi:10.1038/35068596.

39. **Lorenzo IM, Liedtke W, Sanderson MJ, Valverde MA.** TRPV4 channel participates in receptor-operated calcium entry and ciliary beat frequency regulation in mouse airway epithelial cells. *Proc Natl Acad Sci USA* 105: 12611–12616, 2008. doi:10.1073/pnas.0803970105.

40. **Marozkina NV, Gaston B.** Nitrogen chemistry and lung physiology. *Annu Rev Physiol* 77: 431–452, 2015. doi:10.1146/annurev-physiol-021113-170352.

41. **Marozkina NV, Gaston B.** S-Nitrosylation signaling regulates cellular protein interactions. *Biochim Biophys Acta* 1820: 722–729, 2012. doi:10.1016/j.bbagen.2011.06.017.

42. **Marozkina NV, Yemen S, Borowitz M, Liu L, Plapp M, Sun F, Islam R, Erdmann-Gilmore P, Townsend RR, Lichti CF, Mantri S, Clapp PW, Randell SH, Gaston B, Zaman K.** Hsp 70/Hsp 90 organizing protein as a nitrosylation target in cystic fibrosis therapy. *Proc Natl Acad Sci USA* 107: 11393–11398, 2010. doi:10.1073/pnas.0909128107.

43. **McGee KE, Roesch E, Marozkina N, Drumm ML, Hodges CA, Bosch J.** Structurally-driven development of a cross-species, extracellular CFTR antibody (Abstract). *Pediatr Pulmonol* 52: 2017. doi:10.1002/ppul.23838.

44. **McIlwaine MP, Alarie N, Davidson GF, Lands LC, Ratjen F, Milner R, Owen B, Agnew JL.** Long-term multicentre randomised controlled study of high frequency chest wall oscillation versus positive expiratory pressure mask in cystic fibrosis. *Thorax* 68: 746–751, 2013. doi:10.1136/thoraxjnl-2012-202915.

45. **McIlwaine MP, Lee Son NM, Richmond ML.** Physiotherapy and cystic fibrosis: what is the evidence base? *Curr Opin Pulm Med* 20: 613–617, 2014. doi:10.1097/MCP.0000000000000110.

46. **Modena BD, Tedrow JR, Milosevic J, Bleecker ER, Meyers DA, Wu W, Bar-Joseph Z, Erzurum SC, Gaston BM, Busse WW, Jarjour NN, Kaminski N, Wenzel SE.** Gene expression in relation to exhaled nitric oxide identifies novel asthma phenotypes with unique biomolecular pathways. *Am J Respir Crit Care Med* 190: 1363–1372, 2014. doi:10.1164/rccm.201406-1099OC.

47. **Noone PG, Leigh MW, Sannuti A, Minnix SL, Carson JL, Hazucha M, Zariwala MA, Knowles MR.** Primary ciliary dyskinesia: diagnostic and phenotypic features. *Am J Respir Crit Care Med* 169: 459–467, 2004. doi:10.1164/rccm.200303-365OC.

48. **Park JA, Kim JH, Bi D, Mitchel JA, Qazvini NT, Tantisira K, Park CY, McGill M, Kim SH, Gweon B, Notbohm J, Steward R Jr, Burger S, Randell SH, Kho AT, Tambe DT, Hardin C, Shore SA, Israel E, Weitz DA, Tschumperlin DJ, Henske EP, Weiss ST, Manning ML, Butler JP, Drazen JM, Fredberg JJ.** Unjamming and cell shape in the asthmatic airway epithelium. *Nat Mater* 14: 1040–1048, 2015. doi:10.1038/nmat4357.

49. **Prasad BL, Lal R.** A capacitive immunosensor measurement system with a lock-in amplifier and potentiostatic control by software. *Meas Sci Technol* 10: 1097, 1999. doi:10.1088/0957-0233/10/11/321.

50. **Prodromidis MI.** Impedimetric immunosensors–a review. *Electrochim Acta* 55: 4227–4233, 2010. doi:10.1016/j.electacta.2009.01.081.

51. **Ricciardolo FL, Sterk PJ, Gaston B, Folkerts G.** Nitric oxide in health and disease of the respiratory system. *Physiol Rev* 84: 731–765, 2004. doi:10.1152/physrev.00034.2003.

52. **Rosenfeld RJ, Bonaventura J, Szymczyna BR, MacCoss MJ, Arvai AS, Yates JR III, Tainer JA, Getzoff ED.** Nitric-oxide synthase forms N-NO-pterin and S-NO-cys: implications for activity, allostery, and regulation. *J Biol Chem* 285: 31581–31589, 2010. doi:10.1074/jbc.M109.072496.

53. **Seckler JM, Meyer NM, Burton ST, Bates JN, Gaston B, Lewis SJ.** Detection of trace concentrations of S-nitrosothiols by means of a capacitive sensor. *PLoS One* 12: e0187149, 2017. doi:10.1371/journal.pone.0187149.

54. **Shah AS, Ben-Shahar Y, Moninger TO, Kline JN, Welsh MJ.** Motile cilia of human airway epithelia are chemosensory. *Science* 325: 1131–1134, 2009. doi:10.1126/science.1173869.

55. **Shen XM, Zhang F, Dryhurst G.** Oxidation of dopamine in the presence of cysteine: characterization of new toxic products. *Chem Res Toxicol* 10: 147–155, 1997. doi:10.1021/tx960145c.

56. **Sisson JH, Wyatt TA, Pavlik JA, Sarna PS, Murphy PJ.** Vest chest physiotherapy airway clearance is associated with nitric oxide metabolism. *Pulm Med* 2013: 1–6, 2013. doi:10.1155/2013/291375.

57. **Snyder AH, McPherson ME, Hunt JF, Johnson M, Stamler JS, Gaston B.** Acute effects of aerosolized S-nitrosoglutathione in cystic fibrosis. *Am J Respir Crit Care Med* 165: 922–926, 2002. doi:10.1164/ajrccm.165.7.2105032.

58. **Straub AC, Lohman AW, Billaud M, Johnstone SR, Dwyer ST, Lee MY, Bortz PS, Best AK, Columbus L, Gaston B, Isakson BE.** Endothelial cell expression of haemoglobin α regulates nitric oxide signalling. *Nature* 491: 473–477, 2012. doi:10.1038/nature11626.

59. **Stsiapura VI, Bederman I, Stepuro II, Morozkina TS, Lewis SJ, Smith L, Gaston B, Marozkina N.** S-Nitrosoglutathione formation at gastric pH is augmented by ascorbic acid and by the antioxidant vitamin complex, Resiston. *Pharm Biol* 56: 86–93, 2018. doi:10.1080/13880209.2017.1421674.

60. **Swartz MA, Tschumperlin DJ, Kamm RD, Drazen JM.** Mechanical stress is communicated between different cell types to elicit matrix remodeling. *Proc Natl Acad Sci USA* 98: 6180–6185, 2001. doi:10.1073/pnas.111133298.

61. **Whalen EJ, Foster MW, Matsumoto A, Ozawa K, Violin JD, Que LG, Nelson CD, Benhar M, Keys JR, Rockman HA, Koch WJ, Daaka Y, Lefkowitz RJ, Stamler JS.** Regulation of beta-adrenergic receptor signaling by S-nitrosylation of G-protein-coupled receptor kinase 2. *Cell* 129: 511–522, 2007. doi:10.1016/j.cell.2007.02.046.

62. **Wiggs BR, Hrousis CA, Drazen JM, Kamm RD.** On the mechanism of mucosal folding in normal and asthmatic airways. *J Appl Physiol (1985)* 83: 1814–1821, 1997. doi:10.1152/jappl.1997.83.6.1814.

63. **Xu HN, Zhou R, Moon L, Feng M, Li LZ.** 3D imaging of the mitochondrial redox state of rat hearts under normal and fasting conditions. *J Innov Opt Health Sci* 7: 1350045, 2014. doi:10.1142/S1793545813500454.

64. **Xue C, Botkin SJ, Johns RA.** Localization of endothelial NOS at the basal microtubule membrane in ciliated epithelium of rat lung. *J Histochem Cytochem* 44: 463–471, 1996. doi:10.1177/44.5.8627003.

65. **Zaman K, Carraro S, Doherty J, Henderson EM, Lendermon E, Liu L, Verghese G, Zigler M, Ross M, Park E, Palmer LA, Doctor A, Stamler JS, Gaston B.** S-nitrosylating agents: a novel class of compounds that increase cystic fibrosis transmembrane conductance regulator expression and maturation in epithelial cells. *Mol Pharmacol* 70: 1435–1442, 2006. doi:10.1124/mol.106.023242.

66. **Zaman K, Sawczak V, Zaidi A, Butler M, Bennett D, Getsy P, Zeinomar M, Greenberg Z, Forbes M, Rehman S, Jyothikumar V, DeRonde K, Sattar A, Smith L, Corey D, Straub A, Sun F, Palmer L, Periasamy A, Randell S, Kelley TJ, Lewis SJ, Gaston B.** Augmentation of CFTR maturation by S-nitrosoglutathione reductase. *Am J Physiol Lung Cell Mol Physiol* 310: L263–L270, 2016. doi:10.1152/ajplung.00269.2014.

67. **Zhan X, Li D, Johns RA.** Expression of endothelial nitric oxide synthase in ciliated epithelia of rats. *J Histochem Cytochem* 51: 81–87, 2003. doi:10.1177/002215540305100110.